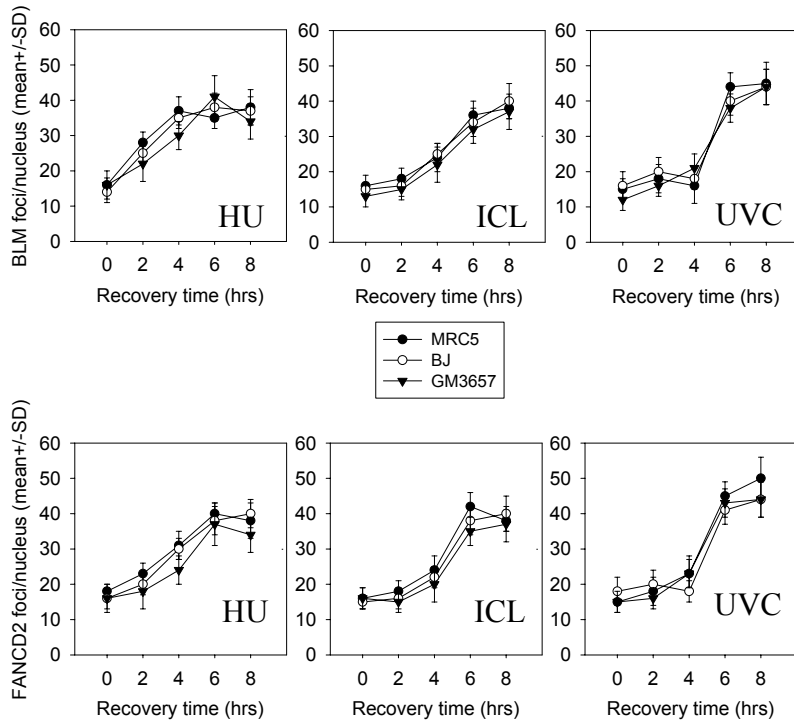
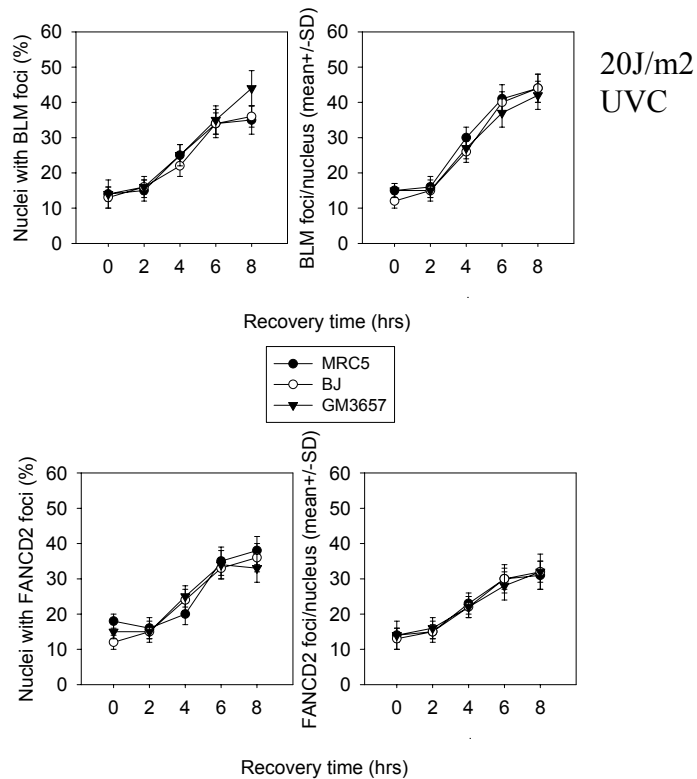


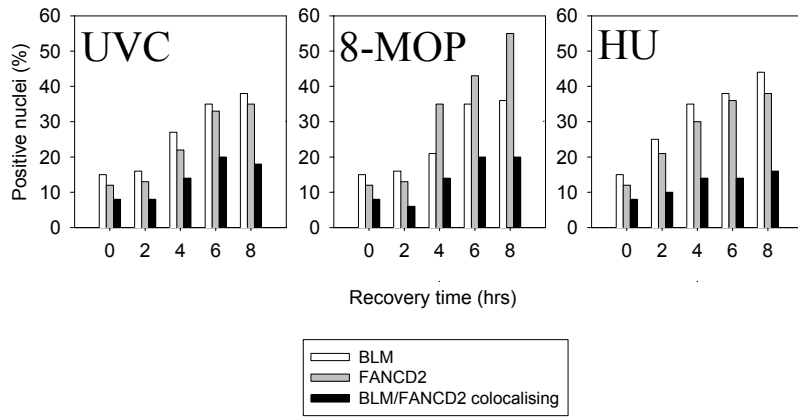
A



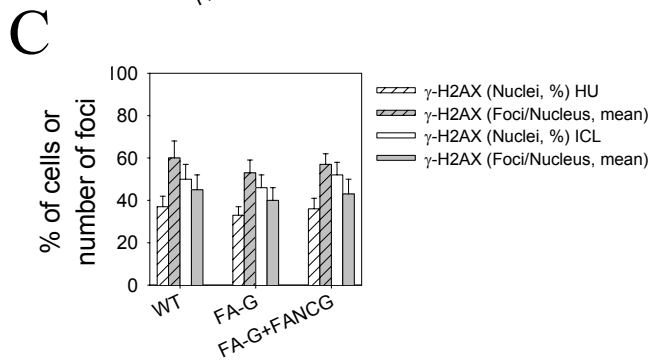
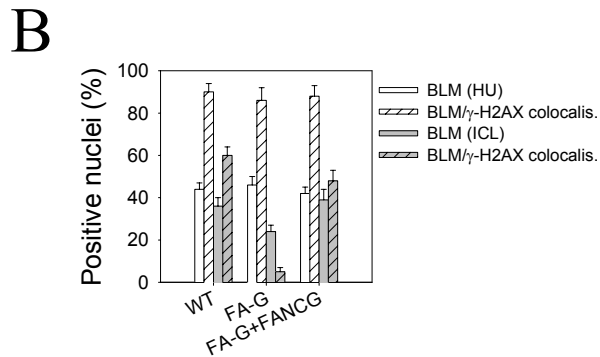
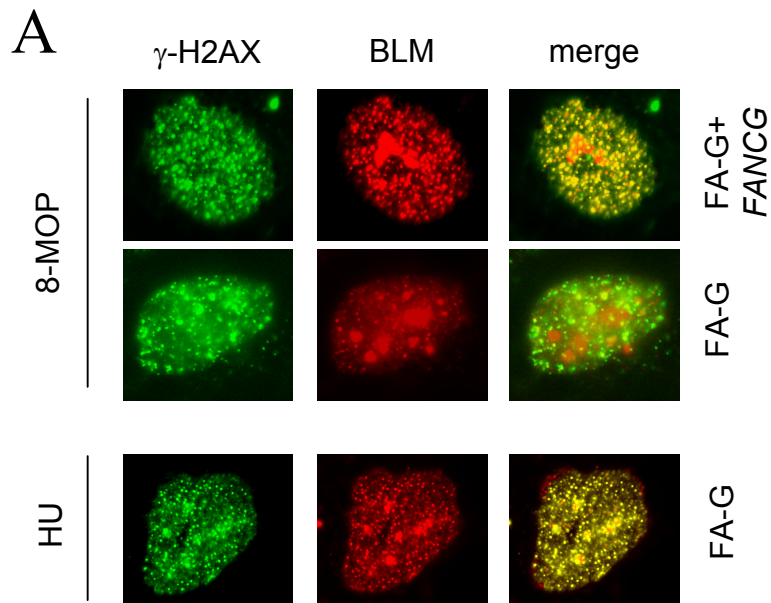
B



Supplementary Figure 1. Evaluation of BLM and FANCD2 accumulation in nuclear foci after ICL or replication arrest. A) ICL- and replication arrest-dependent assembly of BLM and FANCD2 nuclear foci. Wild-type fibroblasts (MRC5 and BJ) and lymphoblasts (GM3657) were exposed to photoactivated 8-MOP (ICL), HU or UVC light and analysed at the indicated time points for the presence of nuclear foci. Data are the mean \pm SD from three independent experiments. B) Wild-type fibroblasts (MRC5 and BJ) and lymphoblasts (GM3657) were exposed to 20J/m² of UVC and analysed at the indicated time points for nuclear foci. The average number of foci derived only from the nuclei positive for focal staining.

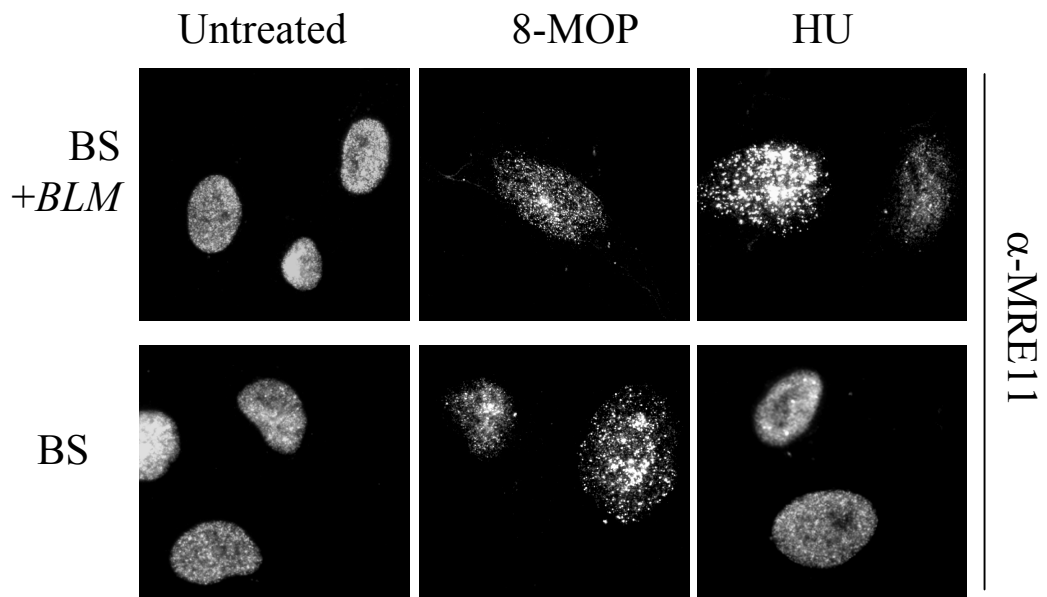


Supplementary Figure 2. Quantification of the BLM/FANCD2 colocalisation. Quantification of the fraction of BLM- and FANCD2-positive nuclei showing colocalisation of the two proteins in MRC5 cells. Data are means from at least three independent experiments, SD are not shown but are always less than 15% of the mean.



Supplementary Figure 3. Analysis of the colocalisation of BLM with the phosphorylated form of the histone H2AX. A) Representative pictures of nuclei immunodecorated for the BLM and the H2AX proteins. Images were taken at 6h post-treatment. Note that BLM/H2AX colocalisation is absent if FA-G cells following ICL treatment but not after HU. B) Quantification of the colocalisation. Cells exposed to photoactivated 8-MOP (ICL) or HU were fixed 6h post-treatment, immunostained and the number of nuclei presenting BLM foci or BLM/H2AX colocalisation recorded. The fraction of nuclei presenting colocalisation is expressed as a percentage of the BLM positive nuclei. The difference between the wild-type and the FA-G cells is statistically significant ($p < 0.01$, Student's T-test). C) Quantification of the H2AX focal accumulation after ICL. The average number of foci derived only from the nuclei positive for focal staining. Data are the mean \pm SD from three independent experiments.

A



B



Supplementary Figure 4. A) MRE11 relocates in nuclear foci in a BLM-independent manner in response to crosslinked DNA. BS and BLM-complemented lymphoblasts were exposed to photoactivated 8-MOP or HU and immunofluorescence carried out 8h later. B) NBS1 is phosphorylated independently to BLM after ICL induction. Cellular extracts from BS and BLM-complemented lymphoblasts exposed to photoactivated 8-MOP (ICL) or HU were prepared 6h after treatment and NBS1 phosphorylation status analysed by Western blotting.

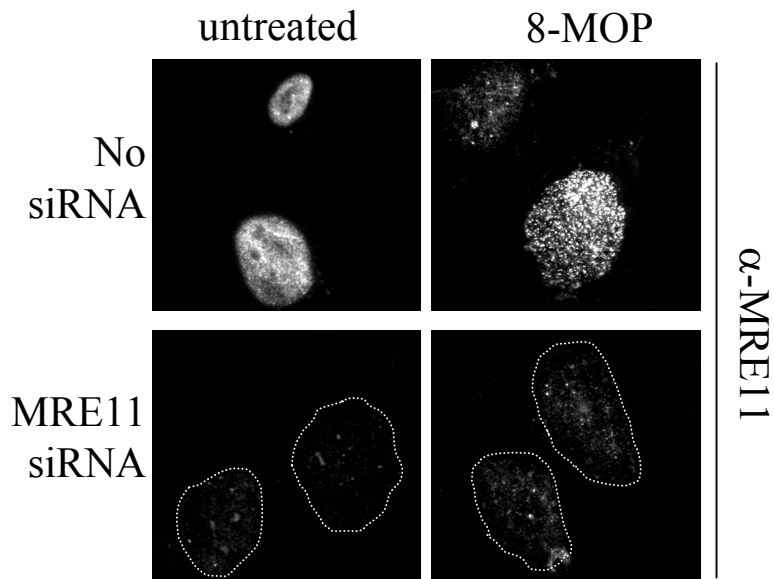
A

	MRE11 –			α-MRE11 WB
	*	–		
GFP siRNA	–	–	+	
MRE11 siRNA	–	+	–	
Untreated	+	–	–	
MRE11 amount	1	0,3	0,9	

B

MRE11 siRNA:	–	–	–	–	+	+
GFP siRNA:	–	–	+	+	–	–
Untreated:	+	+	–	–	–	–
ICL:	–	+	–	+	–	+

C



Supplementary Figure 5. MRE11 RNAi abolished MRE11 complex function. A) MRE11 siRNAs introduction in BS cells inhibited expression of MRE11. hTert-immortalised BS fibroblasts were transfected with siRNAs against MRE11 and cellular extracts assessed for the presence of MRE11 by Western blotting 72h after transfection. The MRE11 level was quantified by densitometry using a cross-reacting band (*) as internal control. The blot is representative of three independent experiments showing consistent results. B) Knock down of MRE11 impaired the functionality of the complex. Wild-type cells transfected with ctrl or MRE11 siRNAs were either left untreated or exposed to photoactivated 8-MOP (ICL) and cellular extracts checked for NBS1 phosphorylation by Western blotting. C) MRE11 expression after RNAi as observed by immunofluorescence. Seventy-two hours after being transfected with siRNAs cells were exposed to photoactivated 8-MOP (ICL) and immunostained for MRE11 8h later.